Decomposition of Nitric Oxide over Barium Oxide Supported on Magnesium Oxide. 2. In Situ Raman Characterization of Phases Present during the Catalytic Reaction

Gerhard Mestl,† Michael P. Rosynek, and Jack H. Lunsford*

Department of Chemistry, Texas A&M University, College Station, Texas 77843

Received: June 23, 1997[⊗]

High temperature in situ Raman spectroscopy was used to determine the complex phase behavior during the decomposition of $Ba(NO_3)_2$ supported on MgO. The starting material, crystalline $Ba(NO_3)_2$, is stable up to 500 °C in a 1% NO in He gas mixture. Above this temperature or at lower NO partial pressures, the crystalline $Ba(NO_3)_2$ is transformed into an amorphous intermediate phase II' which contains nitrate and nitrite ions. This phase is gradually converted into phase II" containing nitrate ions, Ba−nitrito complexes, and the first traces of a Ba−nitro species. The next step in the decomposition is the formation of phase III, which consists mainly of Ba−nitro complexes and nitrate ions. Phase III is stable in decreasing NO pressures until its decomposition into defect-rich BaO, phase IV. A hysteresis was observed for the stability range of phase III as a function of decreasing or increasing NO partial pressures. The transformations between phase III and IV are characterized by isosbestic points in the Raman spectra. Thus, decomposition/reformation of phase III occurs directly without any detectable intermediates. The effect of temperature on the decomposition of phase III into the defect-rich BaO, as determined by Raman spectroscopy, is in good agreement with the calculated coexistence of BaO, BaO_2, and $Ba(NO_3)_2$ phases. Moreover, there is a good correlation between the presence of phase III and the maximum catalytic activity for the decomposition of NO. These in situ Raman results strongly suggest that the observed activity of highly loaded Ba/MgO catalysts arises from the formation of phase III. The sharp falloff in the N_2 formation rate at a particular temperature is related to the transition between phase III and phase IV. Transient in situ Raman experiments indicate that Ba−nitro complexes in phase III are taking part in the catalytic cycle as reaction intermediates.

I. Introduction

Nitric oxide is one of the most ubiquitous pollutants in the atmosphere. It is responsible for the summer smog in urban areas and, thus, for an increasing number of human respiratory system diseases. High ozone concentrations in clean-air areas, far away from urban centers, also arise from urban NO pollution and contribute largely to the dying forest syndrome. Furthermore, NO plays a considerable role in the worldwide greenhouse effect and is also partly responsible for the ozone depletion in the stratosphere.[1−3] Complete removal of NO from off-gases of stationary power plants or from automobile exhausts, thus, becomes an increasing challenge that will require the development of new catalysts.

Barium oxide supported on magnesium oxide (Ba/MgO) catalysts were recently found to be active in catalytic NO reduction by methane.[4] When O_2 was added to the gas feed, the NO conversion increased 3-fold. Using a variable ionization mass spectrometer (VIMS) system, $CH_3^{\bullet}$ radicals were detected in the presence of O_2, but not with NO as the oxidant. Thus, the positive effect of O_2 in catalytic NO reduction was suggested to arise from the generation of $CH_3^{\bullet}$ radicals.

Moreover, the Ba/MgO catalysts exhibited considerable activity for the direct decomposition of NO into N_2 and O_2,[5] a reaction which is very attractive because of the problems associated with the addition of a reducing agent. Particularly interesting catalytic results were observed for the direct NO decomposition when the Ba loadings were 11 mol % or greater.[5] The results of Figure 1 provide a comparison of the catalytic behavior observed during the decomposition of 1% NO in He for MgO containing either 4 or 14 mol % Ba. Up to a certain temperature, defined as the falloff temperature, the rate of N_2 formation was much greater for the 14 mol % Ba/MgO catalyst. At the falloff temperature, a discontinuity in the NO decomposition rate was observed. The discontinuity in rate was accompanied by a large change in the activation energy, which suggests a change in the reaction mechanism. The previous study[5] demonstrated that the falloff temperature increased with respect to increases in NO partial pressure or the presence of added O_2.

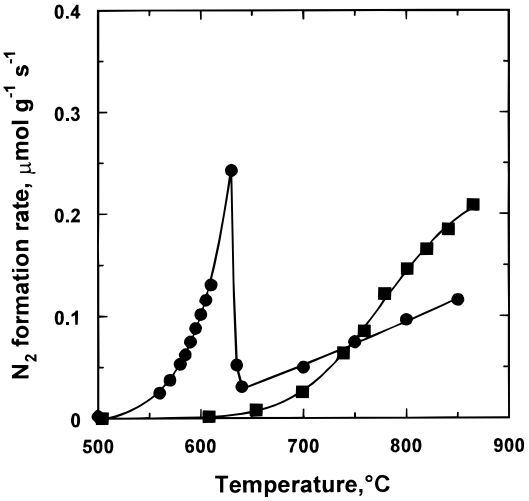

Figure 1. Effect of Ba loading on decomposition of 1% NO/He over Ba/MgO catalysts: ■, 4 mol % Ba/MgO; ●, 14 mol % Ba/MgO.

This paper is the second of a series in which high temperature in situ Raman spectroscopy was used to characterize highly loaded Ba/MgO catalysts prior and during the catalytic decomposition of NO. The series is focused on the 14 mol % Ba/MgO catalyst, because it is representative of the highly loaded materials that exhibit the unique catalytic behavior.[5] In this contribution, in situ Raman spectroscopy is used to define the different phases present in the highly loaded Ba/MgO catalyst.

[⊗] Abstract published in *Advance ACS Abstracts,* October 15, 1997.

S1089-5647(97)02031-2 CCC: $14.00

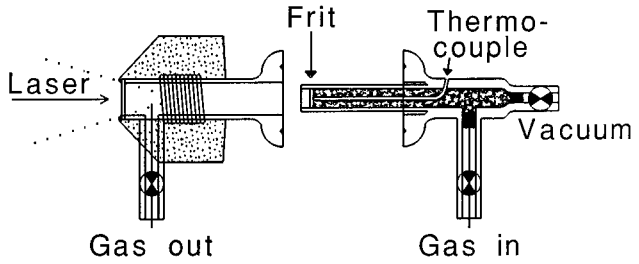

Figure 2. High temperature in situ Raman cell.

The evolution of the exceptional activity for the catalytic decomposition of NO over highly loaded Ba/MgO catalysts will be related to the formation of a special phase containing a Ba−nitro complex. The sharp discontinuity in the catalytic behavior will be shown to result from a phase transition that occurs in the material. The third paper[6] will address the effect of O_2 on the stability of the phases and the species present on these catalysts, while the fourth paper[7] will describe an ^{18}O-isotopic study on the different peroxide species which are observed in these catalytic materials.

II. Experimental Section

The 14 mol % Ba/MgO catalysts were prepared by impregnating MgO (Fisher light, specific surface area 38 m^2/g) with the appropriate amount of $Ba(NO_3)_2$ (Baker). After drying in a rotary evaporator, the material was pressed under 400 kg/cm^2, crushed, and sieved to 20−40 mesh size.

The experimental conditions under which we have studied the changes in the Raman spectra were essentially the same to those used in the catalytic NO decomposition reactions.[5] The total gas flow through catalyst bed (vide infra) was set to 40 mL/min using mass flow controllers (MKS Instruments). The partial pressure of NO (4.1% NO/He, UHP, Matheson) was varied by mixing the gas with pure He (UHP, Matheson).

The Raman spectra were recorded using a Holoprobe spectrometer (Kaiser Optical) equipped with a high performance holographic notch filter to cut off the laser light and an electrically cooled CCD camera with 256 × 1022 pixels. The resolution of this instrument is 5 cm^{-1}, and the wavelength reproducibility is better than 0.5 cm^{-1}. Wavelength calibration was conducted using the emission lines of a standard Ne lamp. The exciting light source is a Nd:YAG laser which is frequency doubled to 532 nm. All Raman spectra were recorded with a low laser power of 2.5 mW, measured at the sample position, to reduce laser heating as much as possible. The exciting laser light is coupled through a quartz fiber to the Raman probe head, which is a telescope with a focal length of 14 cm mounted on a xyz stage (Newport). This design of the Raman probe head holder allows the registration of laterally resolved in situ Raman spectra, with a lateral resolution of about 1 μm. The reproducibility of the positioning with the xyz stage is better than 1 μm. The Raman scattered light is collected in the 180° direction. This *retro*-Raman setup has an advantage in that only one focal plane must be controlled, which is important for high temperature in situ Raman experiments, because it eliminates defocusing due to thermal expansion. There are no moving optical parts in this experimental setup, which together with the high thermal stability guarantees very stable experimental conditions. High temperature in situ Raman spectra of the operating catalyst could be recorded for more than one week without any spurious changes in the base line.

Figure 2 depicts the in situ Raman cell, which was used for this study. It consists of two parts, the cell body and the sample holder. The sample holder is a fused-quartz tube (6 mm i.d.) which fits exactly into the cell body. A frit located below the top of the tube forms a region in which the catalyst powder (ca. 50 mg) is located. This design closely mimics a typical plug flow reactor, and it allows the reaction gases to pass through the catalyst bed. To control the temperature, a thermocouple well is in contact with the lower surface of the frit. The temperature at the catalyst was calibrated prior to the in situ Raman experiments with a second thermocouple placed at the sample position, and under the respective flow of reactant gases, e.g., 1% NO/He. The remaining volume of the sample holder tube is filled with quartz chips, which results in a thorough mixing and preheating of the reactant gases, and the reduction in the dead volume to only 10 mL. The small dead volume allows fast gas-phase response in the cell.

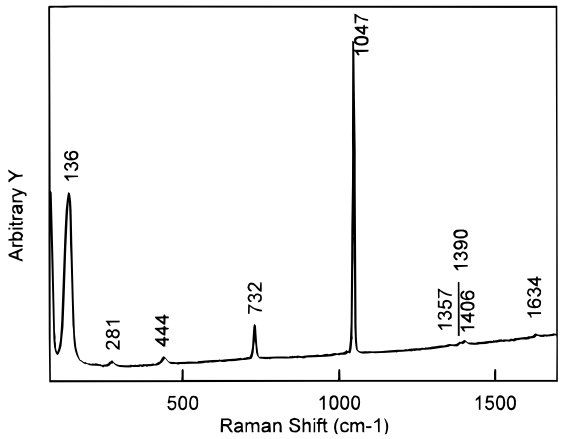

Figure 3. Room-temperature Raman spectrum of 14 mol % $Ba(NO_3)_2$/MgO in He.

The cell body is a fused-quartz tube with an inner diameter of 9 mm. It is closed with a flat optical window. The tube is heated by a tightly wound insulated heating wire (Philips). The heated region is thermally insulated with modified ceramic material (Ceramacast). This combination of heating wire and minimal insulation made it possible to achieve a maximum temperature of 1050 °C with rapid changes in the temperature steps; e.g., an increase of 50 °C could be achieved within 3 min. The small thermal mass resulted in a temperature overshoot for such a temperature step of only 3 °C. In addition, the small thermal mass made possible rapid cooling from the maximum temperature to 100 °C within only 5 min.

III. Results and Discussion

1. Phase Diagram for the Catalyst. The objective of this high temperature in situ Raman study was to determine the species present on the catalyst precursor and those that exist under catalytic conditions. The results indicate that the remarkable decrease in catalytic activity with respect to temperature (Figure 1) is due to a type of phase transition. The term phase is not used in a strict thermodynamic sense because an open system was investigated with material and energy exchange; however, the results indicate that three-dimensional barium compounds are probably present on the MgO.

The Raman spectrum of the precursor catalytic material, composed of $Ba(NO_3)_2$ on MgO, at 25 °C in He is displayed in Figure 3. This spectrum can be fully assigned to crystalline $Ba(NO_3)_2$ which is relatively well crystallized, as revealed by the sharpness of the Raman bands and a narrow Rayleigh line. In addition, the detection of the lattice phonon band at 136 cm^{-1} is proof of crystallinity. Barium nitrate crystallizes in the calcite structure, and accordingly the observed Raman bands are

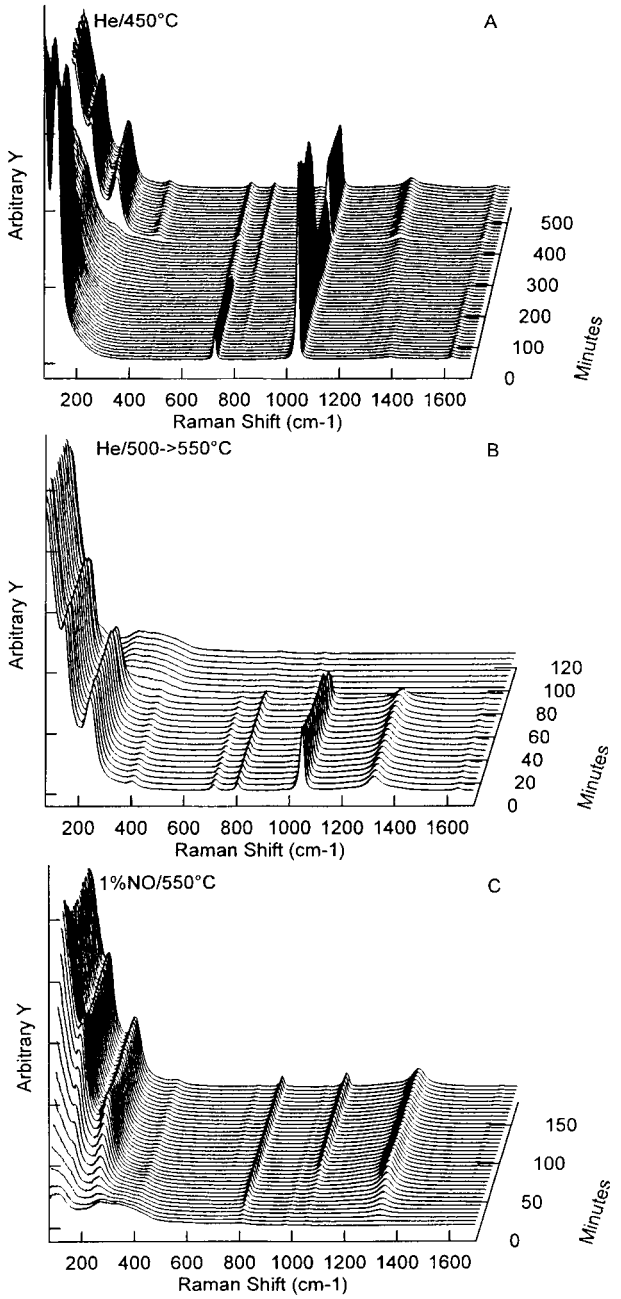

Figure 4. Time-resolved (10 min) in situ Raman spectra obtained during the decomposition of 14 mol % $Ba(NO_3)_2$/MgO in He: (A) Decomposition in He at 450 °C; (B) decomposition in He at 500 for 60 min and then at 550 °C; (C) reaction of the Ba/MgO catalyst with 1% NO at 550 °C.

assigned as follows: the most prominent band at 1047 cm^{-1} is assigned to the symmetric stretching mode of the nitrate ion; the weak band at 1634 cm^{-1} is assigned to the LO, and the group of weaker bands at about 1390 cm^{-1} to the TO modes of the antisymmetric stretch, respectively. The observation of the Raman forbidden antisymmetric stretching modes, on the other hand, confirm that the calcite structure was not perfect. The band of medium intensity at 732 cm^{-1} is assigned to the nitrate bending mode; and the two bands at 444 and 281 cm^{-1} are due to $Mg(OH)_2$, which was found to decompose at 300 °C during catalyst activation.

The series of in situ Raman spectra displayed in Figure 4 shows the changes which occurred in the catalyst material upon increasing the temperature. Series A was recorded at 450 °C with the sample under He. The supported $Ba(NO_3)_2$, (phase I) partially decomposed within 120 min to reach a new stable state, as evidenced by the minor decrease in the intensity of the related Raman bands. During the period of stable NO_3^- intensities, new bands appeared at 810, and 1335 cm^{-1}, which can be assigned to NO_2^- ions by comparison with a reference spectrum of pure $Ba(NO_2)_2$. About 200 min after reaching 450 °C, the Raman spectrum suddenly changed. The lattice phonon band at 126 cm^{-1} completely disappeared, and also the Rayleigh line dramatically lost its intensity. Simultaneously, the intensity of the most prominent Raman band, i.e., the symmetric stretching mode of nitrate, strongly decreased. The changes in the lattice mode regime and in the Rayleigh line indicate the formation of a new, amorphous phase (phase II), which contains NO_3^- and NO_2^- ions. During the next 150 min at 450 °C in He, the intensity of the NO_2^- Raman band at 1335 cm^{-1} further increased together with the slow appearance of a weak shoulder at about 230 cm^{-1}.

After 400 min of reaction at 450 °C in He, another change in the Raman spectra occurred within 10 min. A new band at 1323 cm^{-1} suddenly gained intensity, and, simultaneously, new bands appeared in the lattice mode regime at 143, 244, and 400 cm^{-1}. We assign these bands to the formation of Ba−nitro complexes by comparison with known spectra of transition metal nitro complexes (vide infra). At the same time, the symmetric nitrate stretching mode at 1045 cm^{-1} shifted to 1047 cm^{-1}, while increasing in intensity. These rapid changes in the Raman spectra after certain stable periods are indicative of solid state phase transformations which occurred after certain thresholds or limiting concentrations of the lattice-building ions were reached. Especially, the sudden increase in Raman intensities can only be understood by the formation of a new phase, denoted phase III. Under these conditions, $Ba(NO_3)_2$ is decomposing with the release of O_2, as shown independently by DTA-MS.[8] Thus, one might expect decreasing Raman intensities, in complete contrast to the experimental observations. The newly formed phase III, therefore, must have a larger Raman scattering efficiency than the preceding phase II.

In a separate series of experiments it was shown that phase III finally decomposed after 18 h at 450 °C in He. To accelerate this process in the present experiment, the temperature was increased stepwise to 550 °C with the sample in He. Figure 4B depicts the series of in situ spectra which was recorded during this temperature increase. Phase III was found to be stable at 500 °C for 60 min, but at 550 °C, phase III decomposed within 20 min into phase IV, which is characterized by broad bands in the lattice mode regime (<600 cm^{-1}).

Barium oxide, the final decomposition product, crystallizes in a rock salt structure. First order Raman scattering is symmetry forbidden in this material, but lattice defects in the solid result in the relaxation of the spectroscopic exclusion rule and a weakening of the conservation of momentum condition as well. Hence, the broad Raman bands observed in the lattice mode regime of the spectrum of phase IV can only arise from defect-induced Raman scattering. Therefore, supported BaO, obtained in this manner, must be crystallographically ill defined and contain lattice defects.[7] Weak bands observed in the frequency regime between 700 and 1000 cm^{-1}, in part, can be assigned to peroxide ions,[7] which therefore comprise one type of lattice defect in BaO.

To investigate the effect of an increased NO partial pressure on the stability of phase IV, the gas phase above the catalyst was switched from pure He to 1% NO in He. Series C of the in situ spectra shown in Figure 4 was recorded at 550 °C after switching to NO. Under these conditions defect-rich BaO was not stable and phase III, containing mainly Ba−nitro complexes and NO_3^- ions, was reformed within about 100 min.

In Figure 5, the characteristic Raman spectra are summarized for the four different phases which were observed during $Ba(NO_3)_2$ decomposition in pure He. Both high temperature Raman spectra and room temperature spectra, which were obtained after rapidly cooling the sample, are shown. The material (phase I) after 450 °C is crystalline $Ba(NO_3)_2$ (Figure 5A). The high-temperature spectrum (spectrum a) is characterized by bands at 126, 726, 1046, 1400, and 1632 cm^{-1}, whereas in the room-temperature spectrum (spectrum b), these bands are at higher frequencies due to the thermal effect on lattice parameters. As compared to the spectrum of the starting material (Figure 2), the Raman bands due to $Mg(OH)_2$ are absent.

Magnesium hydroxide decomposes at 300 °C. During the decomposition (spectra not shown), a high fluorescence background first developed in the Raman spectra between 2000 and 3000 cm^{-1}, but subsequently decayed away on the same time scale as the Raman bands related to $Mg(OH)_2$. We, therefore, attribute the low-temperature Raman background to fluorescence associated with basic OH groups.[8] This implies, however, that the high fluorescence levels at high wavenumbers, which were observed in the room-temperature spectra during and after $Ba(NO_3)_2$ decomposition (e.g., spectrum b of Figure 5), must have a different origin. It seems reasonable that this type of fluorescence results from oxygen defects (vacancies) that were formed during decomposition of $Mg(OH)_2$ or $Ba(NO_3)_2$.

The next step in the decomposition was the formation of an amorphous intermediate phase II'. The high-temperature spectrum (a) of Figure 5B shows Raman bands at 725, 810, 981, 1047, and ~1335 cm^{-1}. The peak at 490 cm^{-1} arises from a spurious Hg emission. The room-temperature spectrum b of Figure 5B shows this high fluorescence background (vide supra), on top of which Raman bands are observed at 620, 727, 820, 986, 1055, and 1335 cm^{-1}. The new bands at 620 and 986 cm^{-1} are attributed to the first traces of defect-rich BaO by comparison with the spectra obtained for phase IV (Figure 5F). The most important information from this Raman spectrum is the complete absence of any bands in the lattice mode or metal−ligand vibrational regime, as discussed above. These Raman spectra are attributed to an amorphous phase containing ionic nitrate and nitrite ions.

The next characteristic set of Raman spectra, which were gradually formed with the lapse of time, is exemplified by the two spectra of Figure 5C. The high-temperature spectrum (spectrum a) exhibits bands or shoulders at ~230vw, 715w, 807, 973, 1045, and 1333 cm^{-1}. The room-temperature spectrum (spectrum b) shows more resolution, and bands are detected at 261, 333, 420, 456w, 620, 811, 822sh, 986, 1050, 1059sh, 1235sh, 1335, and 1350sh cm^{-1}. Again, the two bands at 620 and 986 cm^{-1} are attributed to first traces of defect-rich BaO in the catalyst material. The assignment of the other bands observed at this stage of $Ba(NO_3)_2$ decomposition will become evident after considering the set of spectra displayed in Figure 5D, in which the Raman spectra characteristic of phase III are shown.

After heating the sample for 60 min in He at 500 °C, the spectra shown in Figure 5D were observed. The high-temperature spectrum (spectrum a) shows bands at 143sh, 244, 400w, 804, 973, 1047, and 1323 cm^{-1}. In the room-temperature spectrum of Figure 5D (spectrum b), bands are observed at 160, 263, 420, 450sh w, 620w, 718, 807, 821sh w, 903vw, 988, 1049sh, 1060, 1235, and 1323 cm^{-1}. The bands at 620, 903, and 988 cm^{-1} are again attributed to traces of defect-rich BaO. At this stage of decomposition, a band at 903 cm^{-1} is clearly detected and points to an increasing amount of defect-rich BaO in the catalyst material. The Raman bands at 160, 263, 420, 807, 1235sh, and 1323 cm^{-1} are attributed, by comparison with literature values (Table 1), to a Ba−nitro complex species in which the NO_2 ligand is coordinated to Ba via its N atom. The observed bands are assigned following the literature:[9,10] the band at 1323 is the symmetric stretching mode (a_g) of the nitro ligand; the shoulder at 1235 cm^{-1} is the stretching mode of e_g symmetry; and the band at 807 cm^{-1} arises from the NO_2 bending mode. There is some ambiguity in the literature regarding the assignment of the low-frequency Raman bands. If we follow the assignment given by Nolan and James,[9] the band at 420 cm^{-1} would arise from the symmetric Ba−N stretch, while the one at 263 cm^{-1} would be due to the Ba−N stretch of e_g symmetry. Such an assignment would imply that Ba ions are coordinated at least to two nitro ligands. In addition, the symmetric Ba−N stretch would be less intense than the antisymmetric mode of e_g symmetry, which would not be in agreement with general intensity considerations. Because we do not have additional evidence for geminal Ba−nitro complexes (or even higher coordination), we follow the assignment given by Nakagawa et al.[10] and attribute the band at 420 cm^{-1} to the Ba−N stretch, the one at 263 cm^{-1} to a δ_r deformation, and the band at 160 cm^{-1} to a Ba−N deformation mode against a second ligand such as another nitro species, NO_3^-, or O^{2-}.

The remaining set of Raman bands in spectrum b of Figure 5D can be assigned if we consider Figure 5E, in which the characteristic room-temperature spectra of phase II" and III are compared. The bands or shoulders at 333, 456, 822, 1049, and 1350 cm^{-1} in spectrum b of Figure 5C (marked by arrows in Figure 5E) have weak intensity or are even absent in the spectrum of phase III (spectrum b of Figure 5E). Therefore, all of these bands are attributed to a single species in the material. This set of bands is tentatively assigned, by comparison with the literature (Table 1), to a Ba−nitrito complex species, in which the NO_2 ligand is coordinated to Ba via one oxygen. In particular, the band at 1350 cm^{-1} arises from the N═O double bond, and the one at 1049 cm^{-1} from the N−O single bond in the nitrito ligand. The band at 822 cm^{-1} is due to the O−N═O deformation, while the bands at 456 and 333 cm^{-1} can be assigned to the Ba−O stretching and the Ba-ligand deformation modes. The remaining two bands at 718 and 1060 cm^{-1} in the room-temperature spectra of Figures 5C−E, which remain to be assigned, arise from the symmetric stretching and the deformation mode of ionic NO_3^-, respectively. The shift of the symmetric stretch to higher frequencies, and that of the bending mode to lower frequencies, as compared to the starting crystalline $Ba(NO_3)_2$ (Figure 5A), demonstrates that the environment of the nitrate ions has largely changed in the decomposing crystallites.

The last step in $Ba(NO_3)_2$ decomposition is the formation of defect-rich BaO. The spectrum, shown in Figure 5F, is characterized by high-temperature bands and shoulders at 100, 273, 350, 430sh w, 620, 805, and 979 cm^{-1}, and after cooling to room temperature by bands at 200, 278, 338, 400, 450, 517, 620, 790, 818, 894, 930vw, and 987 cm^{-1}. A detailed discussion of the Raman spectrum of defect-rich BaO will be given in a subsequent publication.[7]

In Table 2 the characteristic frequencies for the different species observed during the decomposition of supported $Ba(NO_3)_2$ are listed. In summary, the starting material, phase I, is crystalline $Ba(NO_3)_2$. The first step in decomposition leads to amorphitization of the material and the formation of phase II' which contains mainly ionic nitrates and nitrites. In the progress of decomposition nitrite ions associated with Ba ions become coordinated via the oxygen in phase II". Later, at higher degrees of decomposition, phase III is formed, which mainly

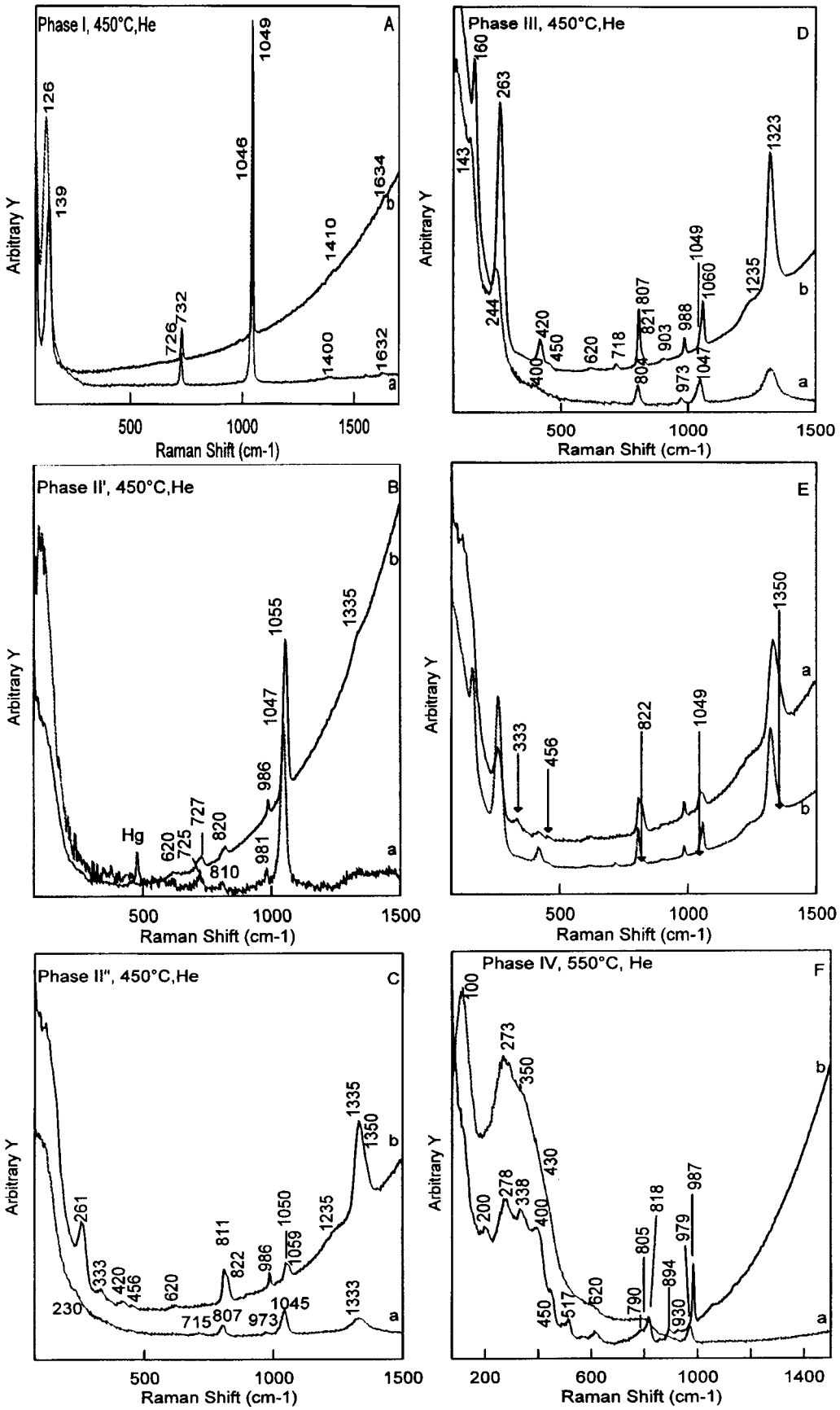

Figure 5. In situ Raman spectra obtained during the decomposition of 14 mol % $Ba(NO_3)_2$/MgO in He: (A) (a) spectrum of phase I at 450 °C in He, and (b) spectrum after cooling to room temperature in He; (B) (a) spectrum of phase II'after 300 min at 450 °C in He, and (b) spectrum after cooling to room temperature in He; (C) (a) spectrum of phase II" after 550 min at 450 °C in He, and (b) spectrum after cooling to room temperature in He; (D) (a) spectrum of phase III after 60 min at 500 °C in He, and (b) spectrum after cooling to room temperature in He; (E) (a) spectrum of phase II" and (b) phase III after cooling to room temperature in He; (F) (a) spectrum of phase IV after 60 min at 550 °C in He, and (b) spectrum after cooling to room temperature in He.

TABLE 1: Vibrational Spectra of Nitro-, Nitrito-, and Chelating NO_2 Complexes (cm^{-1})

$[Pt(NO_2)_6]^{2-}$ [a]	$[Pt(NO_2)_6]^{2-}{}_{soln}$ [a]	$[Co(NO_2)_6]^{3-}$ [b]	$[Co(ONO)]^{2-}$ [b]	$[Co(O_2N)_2(Ph_3PO)]$ [b]
	1322sh	1650 i.r.		
1313	1311	1400 i.r.	1468	
1240	1234	1330		1266
843	840	1250	1065	1199
814	814	826	825	1176
				856
		418/384		
		326		
313	303	293		
286	282			
150	148	150		

[a] Reference 9. [b] Reference 10.

TABLE 2: Raman Bands of Phases and Species Present in 16 mol % Ba/MgO Catalysts (cm^{-1})[a]

phase I	phase II'		phase II''		phase III		phase IV	
nitrate	nitrite	nitrate	nitrito	nitrate	nitro	nitrate	BaO	nitrate
1634			1350		1323			
1410	1335				1235			
1049		1055	1049	1059		1060		1056
							987	
							930	
	820		822		807		894	
							818	
732		727		715		718	790	
							620	
							517	
							450	
			456		420		400	
			333				338	
					263		278	
139					160		200	

[a] Recorded at room temperature in He.

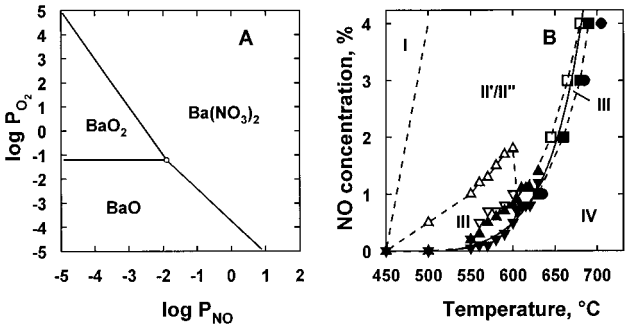

Figure 6. Phase diagrams (A) calculated, and (B) as established by high temperature in situ Raman spectroscopy. In B the solid line is the calculated phase boundary at the triple point between $Ba(NO_3)_2$, BaO_2, and BaO; the dashed lines are the actual phase boundaries as determined by Raman spectroscopy; and (●) are the experimentally observed falloff temperatures in the catalytic decomposition of NO (ref 1); I is crystalline $Ba(NO_3)_2$; II'/II" are amorphous intermediate phases containing NO_3^-, NO_2^-, and Ba−nitrito species; III is an intermediate phase containing NO_3^- and Ba−nitro complexes; IV is a defect-rich BaO phase. Symbols are explained in the text.

contains the Ba−nitro complex. Finally, decomposition occurs into defect-rich BaO (phase IV).

To understand the catalytic behavior,[5] and because there is nothing known about possible phases present and their interconversions under catalytic NO decomposition conditions, we have established a phase diagram for the Ba/MgO material. In Figure 6A, the thermodynamic phase diagram at 590 °C for the $BaO-BaO_2-Ba(NO_3)_2$ system (solid lines) is displayed. This phase diagram was calculated from NIST standard free energy data using the software package HSC (Outokumpu Research Oy, Pori, Finland). There are no NIST data available for $Ba(NO_2)_2$ or the observed intermediate stages of $Ba(NO_3)_2$ decomposition. Therefore, deviations in the actual phase boundaries may be expected. From similar phase diagrams obtained at different temperatures, the calculated triple points between BaO, BaO_2, and $Ba(NO_3)_2$ were obtained, and the results are shown by the solid line in Figure 6B. There is unexpectedly good agreement between these triple point values and the falloff temperatures (filled circles) obtained in the catalytic studies.[5]

Figure 6B also displays the phase diagram, as determined by Raman spectroscopy, which spans NO partial pressures up to 4% and temperatures up to 710 °C. To establish this phase diagram, the 14 mol % Ba/MgO catalyst was stabilized overnight at the respective temperature under 4% NO. Subsequently, the NO partial pressure was lowered stepwise (close to phase transitions, in 0.1% NO steps). At each set of conditions, time-resolved in situ Raman spectra were recorded for a minimum of 1 h to gain information about the stability of the phases and their interconversions. Experimentally determined phase boundaries are indicated by dashed lines in Figure 6B. Phase I, crystalline $Ba(NO_3)_2$, was stable up to 500 °C at the highest NO partial pressures. Above these temperatures or at lower NO partial pressures, it transformed into the amorphous phases II'/II". At still higher temperatures or lower NO partial pressures, the transformation to phase III, which contained the Ba−nitro complex, occurred. Phase III exhibited a hysteresis. For decreasing NO partial pressures, it was stable between the open, downward directed triangles, representing its formation conditions, and the filled, downward directed triangles, representing its decomposition into defect-rich BaO. For increasing NO partial pressures, it was stable between the filled, upward directed triangles, representing its formation, and the open upward directed triangles, representing its transformation to phase II'/II". Above 595 °C, the stability regime of phase III, indicated by the squares, narrowed. The hysteresis, however, between decomposition and reformation of phase III was still observed for temperatures above 595 °C. The close relationship between the observed decomposition of phase III into defect-rich BaO (phase IV), the calculated phase boundary (solid curve), and the falloff temperatures observed in the activity for NO decomposition[5] is the most important information which is drawn from this phase diagram. These observations strongly suggest that the catalytic activity exhibited by these highly loaded Ba/MgO catalysts and the observed sharp falloff in N_2 formation rate are related to the formation of phase III and the transition between phase III and phase IV, respectively.

This suggestion was corroborated by a separate series of in situ Raman experiments,[5] and the spectra are reproduced in Figure 7. In series A, spectra were recorded with the catalyst under 1% NO/He after the temperature was increased from 625 °C to 630 °C. At 625 °C, phase III was present. After a temperature of 630 °C was reached, the Ba−nitro phase III

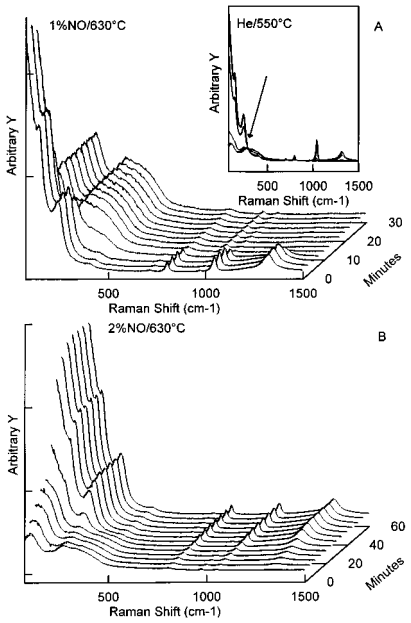

Figure 7. Time-resolved (5 min) high temperature in situ Raman spectra showing the transformation between phases III and IV: (A) decomposition of phase III containing mainly Ba−nitro species into defect-rich BaO in 1% NO/He at 630 °C; (B) reformation of phase III at the same temperature under 2% NO/He. Insert: Decomposition of phase III into phase IV that occurs via an isosbestic point.

decomposed within 5 min into defect-rich BaO. The NO partial pressure was then increased to 2% NO/He at the same temperature, and series B was recorded. The spectra show that phase III, containing the Ba−nitro complexes, reformed from defect-rich BaO within 30 min. At this higher NO partial pressure, decomposition into defect-rich BaO was again observed after the temperature was raised to 645 °C (spectra not shown). These transformations between phase III and IV occurred via isosbestic points as shown in the insert of Figure 7. This observation demonstrates that the decomposition/reformation occurs directly without any detectable intermediates.

To summarize, a complex phase behavior is correlated with the unusual catalytic behavior of the 14 mol % Ba/MgO sample. Phase III is stable under catalytic conditions, and the sharp falloff in N_2 formation can be correlated with the decomposition of phase III to phase IV, which is composed of defect-rich barium oxide. This phase transformation occurs via an isosbestic point in the related in situ Raman spectra. The catalytically relevant phase III contains mainly Ba−nitro complexes, nitrates, and traces of defect-rich BaO.

2. Reaction Intermediates and Related Species. To determine which, if any, of the three species present in phase III was an intermediate in the NO decomposition reaction, transient catalytic and in situ Raman experiments were carried out, and the results are reported in part 1.[5] Briefly, the catalyst was stabilized overnight at the particular temperature under 4% NO. Then, the NO partial pressure was lowered in one step to a value at which phase III, containing mainly the Ba−nitro species, should be formed. The temperatures of these experiments were 590, 575, 550, 625, and 650 °C, in this order. At 590 °C, for example, under 4% NO, phase II" was stable, and contained nitrite, Ba−nitrito, and traces of Ba−nitro species (Figure 8A). The band at 1336 cm^{-1} related to the Ba−nitrito species completely vanished 10 min after switching from 4% to 0.5% NO. A new band characteristic of the Ba−nitro complex appeared at 1322 cm^{-1}. Its formation required about 30 min. Meanwhile, on the same time scale the catalytic activity increased to a new steady-state level (see Figure 6, part 1[5]).

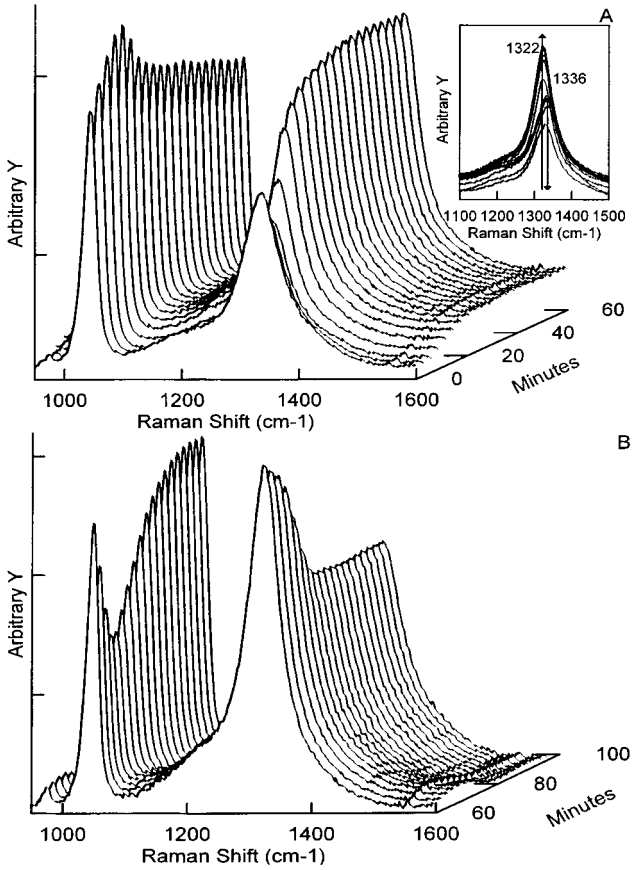

Figure 8. Time-resolved (3 min) transient in situ Raman spectra at 590 °C: (A) after switching the gas-phase concentration of NO from 4% to 0.5%; (B) after switching the gas phase concentration of NO from 0.5% to 4%. Insert: Decrease of the Ba−nitrito stretching mode at 1336 cm^{-1} and increase of the Ba−nitro stretching mode at 1322 cm^{-1} after switching the gas-phase concentration of NO from 4% to 0.5%.

The process was reversible (Figure 8B) in that a change from 0.5 to 4% NO caused the Ba−nitro complex to disappear and the original steady state activity was recovered.[5] This series of combined transient catalytic results and time resolved in situ Raman spectra strongly suggest that the Ba−nitro complex is directly involved in the catalytic cycle.

The intensity of the Raman bands related to nitrates, depicted in Figure 8, showed an unusual behavior in that they went through a maximum upon decreasing the NO pressure and through a minimum upon increasing the NO pressure. These intensity variations were not in agreement with the changing catalytic activities in the transient experiments.[5] Therefore, it is suggested that nitrates are only indirectly related to the catalytic NO decomposition. Still, it is of interest to understand this unusual intensity behavior.

In the following series of in situ Raman experiments, the temperature was lowered to 500 °C in order to slow the reactions. At this temperature, the gas phase above the catalyst was switched between 0.1% NO and pure He. At 500 °C and 0.1% NO, phase III containing mainly the Ba−nitro complexes was stable. After switching to pure He, where decomposition into BaO occurs, the nitrate stretching band showed a rapid intensity reduction, but the intensity of this band increased, again over ca. 100 min under He as shown in Figure 9A. During the same time period, the intensity of the Raman bands related to Ba−nitro complexes decreased monotonically. Both Raman signals reached a stable state that remained until 200 min on stream. After this period, decomposition finally occurred and both bands disappeared.

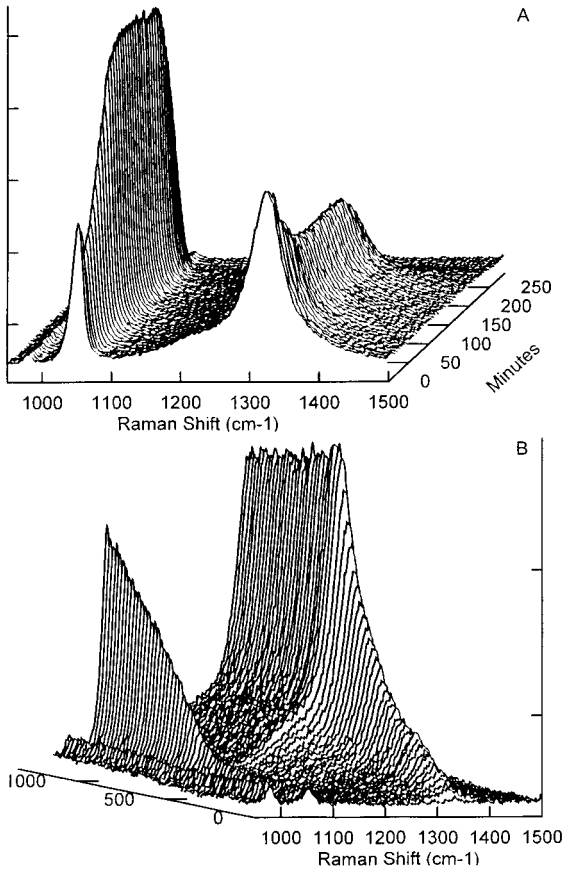

Figure 9. Time-resolved (10 min) transient high temperature in situ Raman experiments at 500 °C: (A) after switching the gas-phase concentration of NO from 0.1% to pure He; (B) after switching the gas phase from pure He to 0.1%NO/He.

When the gas phase was switched back from pure He to 0.1% NO (Figure 9B), the band, related to the Ba−nitro complex, immediately gained intensity. The stretching band at 1056 cm^{-1} of the remaining bulk nitrate ions, however, remained weak for 500 min. Only after the band due to Ba−nitro complexes reached its maximum intensity did the nitrate-related Raman band start to increase in intensity.

The observation in Figure 9A that the nitrate band mainly increased while the Ba−nitro band decreased may be understood by assuming that the partial decomposition of the nitro species produces N_2 and O_2. Oxygen reacts with some of the remaining nitro species to produce more nitrate ions. This reaction will be described more fully in the subsequent paper of this series.[6]

IV. Summary and Speculation about the Reaction Mechanism

In our previous publication[5] we reported on the activation energies for NO decomposition over Ba/MgO catalysts. The high catalytic activity, observed for extensively loaded Ba/MgO catalysts ($\geq$11 mol % BaO) was characterized by an activation energy of 47 kcal/mol. At temperatures above the sharp falloff in NO conversion, and for low loaded catalysts, the activation energy was 13 kcal/mol. The catalytic results also revealed that N_2O is not involved in the NO decomposition below the falloff temperature, whereas it was found to be an intermediate in the high-temperature reaction. These facts suggest that there are two different reaction mechanisms depending on temperature, NO partial pressure, and Ba loading.

For the highly loaded Ba/MgO catalysts, in situ Raman spectroscopy provides information on the complex phase behavior during $Ba(NO_3)_2$ decomposition. After impregnation and drying, the crystalline $Ba(NO_3)_2$ phase is present and no traces of amorphous $Ba(NO_3)_2$ surface species, carbonates, or $Ba(OH)_2$ were observed. The crystalline $Ba(NO_3)_2$, is stable up to 500 °C at the highest NO partial pressures employed. Above these temperatures, or at lower NO partial pressures, it transforms into the amorphous intermediate phases II'/II", which contain mainly nitrate and nitrite ions and Ba−nitrito species. The next step in decomposition is the formation of phase III, which consists of nitrate ions and mainly Ba−nitro complexes. The Ba−nitro complex containing phase III is stable in decreasing NO pressures until its decomposition into BaO. In pure He, this decomposition into BaO occurs after extended time periods at temperatures as low as 450 °C. The relationship between the phases is illustrated in Scheme 1, part 3 of this series.[6]

The formation of phase III, containing mainly the Ba−nitro species, occurs under conditions at which the catalytic activity is observed for highly loaded Ba/MgO catalysts.[5] The decomposition of phase III into defect-rich BaO closely follows the calculated *loci* of points at which BaO, BaO_2, and $Ba(NO_3)_2$ coexist. Moreover, there is agreement between the maximum temperature for phase III and the falloff temperatures observed in the catalytic reaction.[5] These results strongly suggest that the observed sharp falloff in N_2 formation rate is related to the phase transition between phase III and phase IV.

The knowledge of the phase relations was necessary to develop a consistent picture of the reactions which occur under the conditions at which the extra catalytic NO decomposition was detected over highly loaded Ba/MgO. Transient experiments convincingly demonstrate that the Ba−nitro complexes are taking part in the catalytic cycle as reaction intermediates. The intensity of the Raman bands of these Ba−nitro complexes show a behavior upon changes in the gas-phase NO concentration which is consistent with the catalytic data:[5] their concentration increases on the same time scale as the catalytic activity increases and *vice versa*. By contrast, the intensity variations of the Raman bands related to NO_3^- or Ba−nitrito species are not in agreement with the changing catalytic activities in the transient experiments. Accordingly, these species are only indirectly related to the catalytic cycle. Phase II'/II'', however, seems to act as a buffer for the active Ba−nitro intermediates when the NO concentrations above the catalyst are varied.

Acknowledgment. This research was supported by the National Science Foundation under Grant No. CHE-9520806. G. Mestl had a Feodor-Lynen-Research Fellowship provided by the Alexander von Humboldt Foundation.

References and Notes

(1) Wojtowicz, M. A.; Pels, J. R.; Mouljin, J. A. *Fuel Process. Technol.*, **1993**, *34*, 1.

(2) Elkins, J. W.; Rossen, R. *Summary Report 1988*: Geophysical monitoring for climatic change, NOAA ERL, Boulder, **1989**.

(3) Houghton, J. T.; Jenkins, G. J.; Ephraums, J. J. (Eds.), *Climate Change, The IPCC Scientific Assessment*, Press Syndicate of the University of Cambridge, London, 1990.

(4) Xie, S.; Rosynek, M. P.; Lunsford, J. H. *Catal. Lett.*, **1997**, *43*, 1.

(5) Xie, S.; Mestl, G.; Rosynek, M. P.; Lunsford, J. H. *J. Am. Chem. Soc.*, in press.

(6) Mestl, G.; Rosynek, M. P.; Lunsford, J. H. *J. Phys. Chem.*, 1997, *101*, 9329.

(7) Mestl, G.; Rosynek, M. P.; Lunsford, J. H. *J. Phys. Chem.*, submitted.

(8) Jeziorowski, H.; Knözinger, H. *Chem. Phys. Lett.* **1977**, *51*, 519.

(9) Nolan, M. J.; James, D. W. *Aust. J. Chem.* **1970**, *23*, 1043.

(10) Nakagawa, I.; Shimanouchi, T.; Yamasaki, K. *Inorg. Chem.* **1964**, *3*, 772.

(11) Nakamoto, K. *Infrared Spectra of Inorganic and Coordination Compounds*, 2nd ed., Wiley Interscience: New York, 1970; p 160f.